AN INSTANTANEOUS OPTIMIZATION BASED POWER MANAGEMENT STRATEGY TO REDUCE FUEL CONSUMPTION IN HYDRAULIC HYBRIDS

Rajneesh Kumar and Monika Ivantysynova

Purdue University, Department of Mechanical Engineering, Maha Fluid Power Research Center, 1500 Kepner Drive, Lafayette, IN 47905, USA
rajneesh@purdue.edu, mivantys@purdue.edu

Abstract

An instantaneous optimization based power management strategy for output-coupled power-split based hydraulic hybrids has been described in this work. Design considerations for a hydraulic accumulator based regenerative system for hybrids have been outlined. Optimal operation of the non-hybrid version of the power-split transmission provides useful insight into the system optimization and its result has been utilized later.

Instantaneous optimization based control combines the efficient system operation with the braking energy regeneration to achieve fuel savings with the hydraulic hybrids in this work. Fuel mileage for a hybrid passenger car has been simulated for standard drive cycles under the instantaneous optimization based control.

An output-coupled power-split transmission prototype built on the Hardware-In-the-Loop (HIL) principle has been described briefly. Proposed instantaneous optimization based control has been implemented on the test-rig. The proposed management strategy is compared through measurements and simulations to validate its effectiveness in improving fuel economy.

Keywords: hydraulic hybrids, fuel economy, instantaneous optimization, power management, hardware-in-the-loop

1 Introduction

Powertrain hybridization is a proven concept for improving the fuel economy in all automotive as well as off-road applications. Indirectly, by burning less fuel it also reduces emissions and helps meet the stringent emission norms. Hybridization can be achieved through diverse technologies, such as electrical, mechanical and hydraulic. The nature of the technology reflects how the braking energy is stored in the regenerative system. An electric hybrid would be equipped with, for example, an electrical battery or a bank of ultra-capacitors with associated power electronics pack that captures and stores energy as electrical energy. A flywheel on the other hand stores braking energy as kinetic energy. Hydraulic hybrids in this regard have achieved significant attention recently.

Environmental Protection Agency (2006) demonstrated that a prototype series hydraulic hybrid UPS delivery truck achieves 60 - 70 % better fuel economy and 40 % or more reduction in CO_2 in laboratory tests compared to the baseline vehicle. Artemis Intelligent Power Ltd (2006) equipped a prototype BMW 530i with its Digital Displacement Hybrid Transmission which is a hydraulic series hybrid. It was reported that the prototype BMW 530i gave double the fuel mileage in city driving compared to the same car with a six speed manual transmission while it cut down the CO_2 emissions by approximately 30 %. Hydraulic hybrids have proved particularly useful for heavier applications in stop-and-go kind of scenario. Examples would include refuse trucks, delivery vans and city buses. Significant amount of fuel can be saved given the extent of braking energy available during typical drive cycles and the sheer fleet size of these commercial vehicles. For such applications, there is a burst of energy to be captured that needs to be released quickly during the next acceleration period. High power density of hydraulic components and charging-discharging characteristics of hydraulic accumulators make the hydraulic hybrid powertrain a viable option.

There have been many attempts to build hydraulic hybrid prototypes for heavy duty applications. Machinenfabrik Augsburg-Nuernberg Ag. (MAN) in Berlin, Germany (Martini, 1984) built Hydrobus I with hybrid parallel configuration and recorded a fuel saving of 25 % around inner city Berlin. The MAN Hydrobus II

This manuscript was received on 01 October 2010 and was accepted after revision for publication on 14 June 2011

used a hybrid power-split configuration with a downsized diesel engine. Fuel savings were recorded at around 18 to 33 % in comparison to the standard MAN bus. Mitsubishi Motors Japan (Nakazawa et al., 1987) developed the Braking Energy Storage and Regeneration System (BER System) for installation onto Japanese city buses. BER system utilized the power-assist (parallel) layout and was installed with a downsized engine. In dynamometer testing, the BER buses recorded fuel saving of 30 % over the standard buses. Hugosson (1993) describes the development of Cumulo Brake Energy Drive (CBED), which is a parallel type hydraulic hybrid. It recorded an average reduction in fuel consumption at 16 to 25 % for normal operation. The main focus of his paper was Cumulo Hydrostatic Drive (CHD), a series type hydraulic hybrid. Results gathered from dynamometer testing over a range of trapezoidal start-stop driving cycles showed a potential fuel saving of 48 % for the CHD series version and 35 % for the CBED parallel version. The parallel hydraulic hybrid system on a 9700 kg city bus developed by the Canadian NRC (1989) registered a 19 % improvement in fuel economy, on a 48 km/h constant speed cycle with 3 stops per kilometrmile, over the baseline vehicle. Dynamometer testing found significant reduction in NOx, particulate and CO emissions.

Continuously variable transmissions (CVT), in general, suffer from poor transmission efficiency. A power-split transmission is a class of CVT that combines a highly efficient mechanical transmission with a continuously variable part using a planetary gear train (PGT). Depending on the type of variable path, a general schematic of power split is shown in Fig. 1.

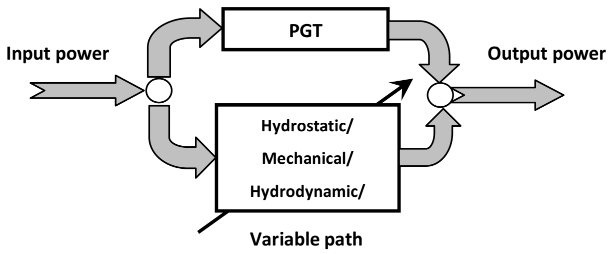

Fig. 1: *Power-split general scheme*

In this work, the CVT part has been realized through a hydrostatic transmission. With a proper control strategy, power-split can offer the advantages of series and parallel layouts without suffering from their shortcomings. In power split, like series hybrid, engine operation is independent from the wheels and hence can be managed to operate in its most optimal region. But owing to the parallel mechanical path of power transfer, the overall transmission in power split is more efficient than purely hydrostatic drive. Also, similar to the parallel configuration, mechanical and hydraulic power paths in power split are capable of driving the vehicle individually or in power-additive mode. Power-split based transmission itself can be classified into simple configuration consisting of a single planetary gear train (PGT) and more complex architectures consisting of twin planetary systems. In its simplest configuration, a power-split transmission can either be of input coupled or output coupled type depending on which side of the transmission CVT is connected to.

A thorough review of power-split based CVTs in the agricultural market can be found in Renius and Resch (2005). Power-split based transmission for city-bus application and the fuel saving benefits of powertrain hybridization is the subject of investigation of Bowns et al. (1981) and Dorey and Vaughan (1984). It is a seminal work on the modeling, sizing and analysis of the power-split based hydraulic hybrids. Results from their research shows that hybrid power-split can improve the fuel economy by 27.7 % compared to a conventional bus.

Having another energy source on-board adds to the complexity of the powertrain but it also opens up new opportunities to manage the entire powertrain in a more energy-efficient manner. Effective decoupling of the engine speed from the wheel speed and energy storage on-board provide extra degrees of freedom when it comes to controlling the engine and the transmission to fulfill the overall goal of achieving higher fuel economy. To harness these benefits, however, a comprehensive control strategy is needed. Control concepts ranging from the rule-based approach to the ones guaranteeing optimality have been explored in the literature.

Power management of power-split based hydraulic hybrids has not received its share of attention in the literature. Work in this paper is aimed at designing a practical and implementable supervisory level control that, although sub-optimal, improves the fuel economy of power-split based hydraulic hybrids substantially. A truly optimal power management solution requires the knowledge of future drive cycle and hence will be of little practical value.

Sizing of a hydraulic accumulator for a passenger car type application is described in the next section. Bulk of the work in this paper is devoted to the development of the instantaneous optimization based power management. Experimental validation of the practicality, ease of application and effectiveness in improving fuel economy of the proposed approach comes from a prototype testing. Brief description of the experimental set-up is provided before comparing the simulation and measurement results for a sample drive cycle.

2 Sizing of the Regenerative System

For small to medium power applications, an output coupled power-split transmission is well suited because of its fairly steady efficiency curve, relative compactness, simple structure and low control effort.

The layout of a hybrid OCPSD is shown in Fig. 2.

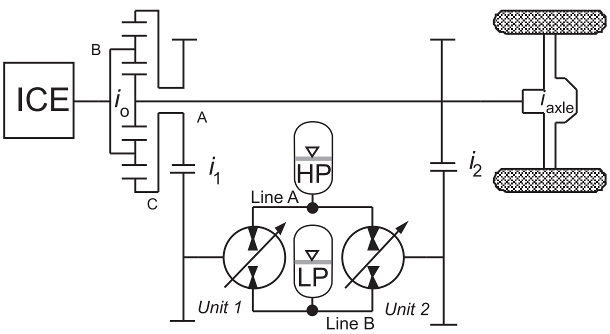

Fig. 2: *Hybrid output coupled power split drive*

While designing a regenerative system for any application, particularly for a passenger car owing to space constraint, it is desirable to arrive at the smallest possible size. Braking energy storage capacity of the accumulator not only directly affects the fuel economy achievable with a hybrid powertrain but is also responsible for determining the acceleration and braking performance of the drivetrain; as explained later. Therefore, careful attention has to be paid to the sizing of the regenerative system.

Two most important issues in the design of a regenerative transmission are the level of braking that is required and the amount of energy that is available for recovery. Desired level of deceleration in every braking scenario is achieved by the proper manipulation of pressure level in the accumulator. This will be the topic of discussion in the section on power management. The accumulator needs to be sized to capture a certain percentage of available braking energy during a representative drive cycle.

Plot of a representative drive cycle for a passenger vehicle type of application is shown in Fig. 3. It combines many Environmental Protection Agency (EPA) Dynamometer Driving Schedules representative of urban, suburban and highway driving and captures the essential driving characteristics in a wide range of scenarios.

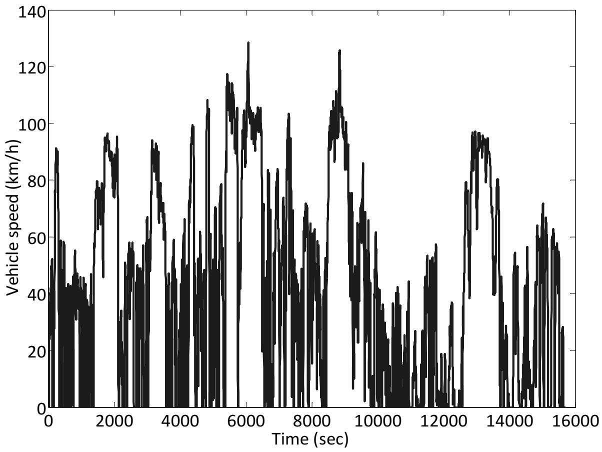

Fig. 3: *Representative drive cycle for a passenger vehicle*

Based on this drive cycle, for each of the braking events the energy available for recovery has been calculated. A braking event lasts from the onset of braking initiated by the human driver till he/she releases the brakes. To compute the recuperable energy, E_{cap}, during each such event that lasts from t_1 to t_2, energy consumed in overcoming drag, rolling resistance and grade has been subtracted from the braking energy, as shown in Eq. 1.

$$E_{\text{cap}} = \sum_{t_1}^{t_2} \left\{ M_{\text{br,wh}} - (F_{\text{drag}} + F_{\text{fric}} + F_{\text{grade}}) \right\} \gamma \tag{1}$$

List of vehicle parameters, typical for a passenger car, is shown in Table 1. These values are used in all the sizing and simulation exercises.

Table 1: Vehicle parameters

Vehicle mass	1311	Kg
Coefficient of drag (C_d)	0.26	-
Frontal area (A)	2	m^2
Tire radius (r_{tire})	0.305	m
Coefficient of rolling resistance (C_r)	0.015	-

Figure 4 shows the available energy during each braking event in ascending manner. An accumulator sized to capture 90 % of the total energy will have the capacity to store 0.271 MJ in a single braking event, as indicated on the plot in Fig. 4.

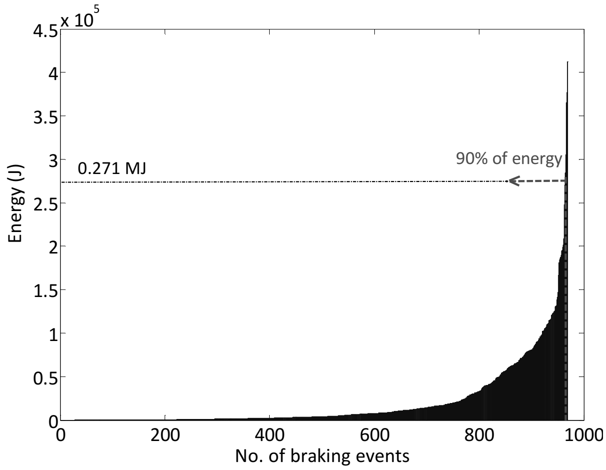

Fig. 4: *Braking energy distribution for braking events*

An indirect way of estimating the accumulator capacity is found by analyzing the histogram of braking energy. Figure 5 shows the distribution of available braking energy as a function of vehicle speed. As indicated on the plot, 90 % of the energy is contained within 0 to 78 km/h.

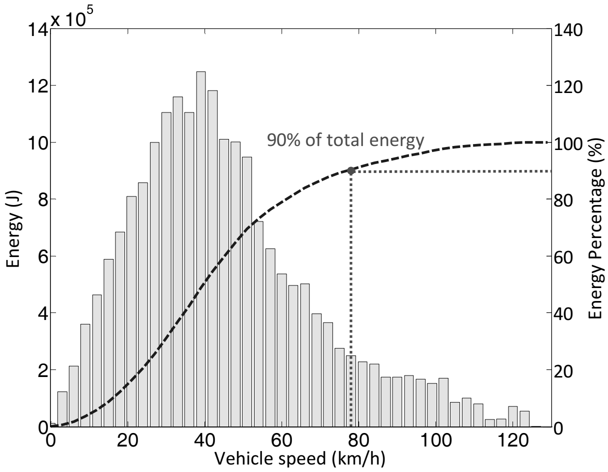

Fig. 5: *Braking energy distribution as a function of vehicle speed*

Distribution of available energy at 78 km/h as a function of deceleration level is shown in Fig. 6. As seen, all the energy can be captured by achieving a maximum braking rate of 2.4 m/s^2. Therefore, assuming that vehicle is brought to stop from 78 km/h by applying a braking force that results in a deceleration level of 2.4 m/s^2, the available energy the accumulator needs to be sized for is computed to be 2.817×10^5 J = 0.282 MJ. This estimate of accumulator storing capacity based on the vehicle kinetic energy is slightly conservative since the accumulator need not store all the available energy at 78 km/h to ensure at least 90 % energy capture during the entire drive cycle. In fact, even if sized based on storing 0.271 MJ, the accumulator will be able to capture more than 90 % of total energy. It will be possible to store part of the available energy for some braking events shown in Fig. 4 that feature more energy than the storing capacity of accumulator by applying a combination of friction and hydraulic brakes. Therefore, accumulator sizing is based on the 0.271 MJ energy storage criterion.

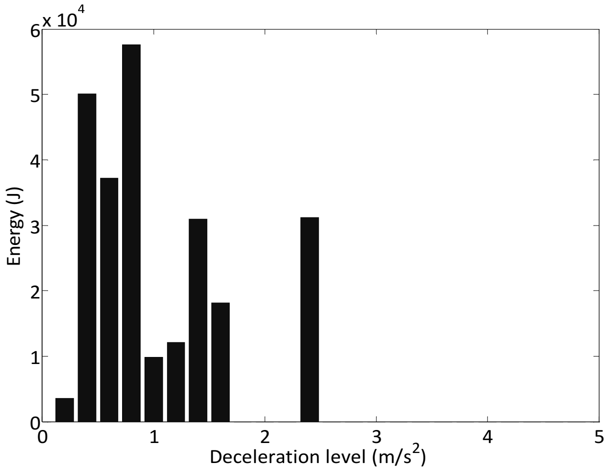

Fig. 6: *Braking energy distribution at 78 km/h vehicle speed*

Assuming the charging or discharging of the accumulator follows an adiabatic process, pV^n = const., the expression for energy stored in a charging process where gas pressure and volume are taken from p_1, V_1 to p_2, V_2 is given by Eq. 2.

$$\begin{aligned} E_{\mathrm{acc}} &= \int_{V_1}^{V_2} p dV \\ &= \int_{V_2}^{V_2} \frac{const.}{V^n} dV \\ &= const. \left[\frac{V^{1-n}}{1-n} \right]_{V_1}^{V_2} \\ &= \frac{const.}{1-n} \left[V_2^{1-n} - V_1^{1-n} \right] \end{aligned} \tag{2}$$

The polytropic index of n = 1.4 assuming nitrogen gas at 15 °C and 1 atm pressure undergoing adiabatic process has been used. Defining the ratio between minimum working pressure p_1 and maximum allowable pressure p_2 as r, i.e. $r = p_1/p_2$, and after some algebraic manipulations, expression for energy storage in the accumulator is reduced to,

$$E_{\mathrm{acc}} = \frac{p_2 (r^{1/n} - r)}{(1-n)} V_1 \tag{3}$$

E_{acc} is the maximum energy that can be stored in an accumulator that operates between the given pressure range p_1 to p_2. Equating E_{acc} to the maximum braking energy E_b = 0.271 MJ that needs to be stored during the hardest braking event, expression for the maximum gas volume V_1 in the accumulator is given by Eq. 4.

$$V_1 = \frac{(1-n) E_b}{p_2 (r^{1/n} - r)} \tag{4}$$

Assuming the maximum operating pressure to be p_2 = 380 bar, V_1 has been plotted as a function of the minimum pressure p_1 in Fig. 7.

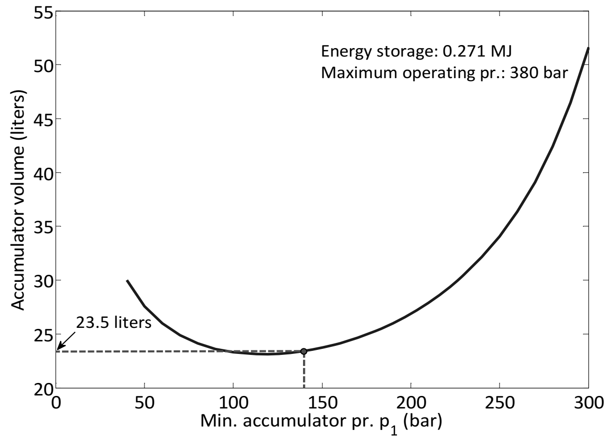

Fig. 7: *Accumulator capacity as a function of minimum pressure*

From the plot in Fig. 7, the smallest accumulator size is 23.13 liters for p_1 = 120 bar. It would be beneficial for acceleration and braking performance to keep the minimum working pressure in the accumulator slightly higher without sacrificing the accumulator size much. Therefore, at p_1 = 140 bar, a 23.5 liter accumulator is selected. It is noteworthy that if the accumulator was sized to capture at least 95 % of the total energy, instead of 90 %, its size will have to increase from 23.5 liters to 31.5 liters. The slight increase in captured energy does not justify such a jump in the accumulator size for a passenger car kind of application. There is, however, another merit behind choosing a bigger size accumulator for capturing a certain amount of energy. From Fig. 7 it is obvious that minimum pressure p_1 can be raised further if a bigger size accumulator is selected. It will be shown in the power management section that accumulator pressure directly affects the driving performance and a higher value of p_1 makes it easier to meet the driving performance while capturing all the required energy. But it comes at a price; bigger accumulator size. It takes careful manipulation of the accumulator pressure to ensure maximum energy storage without compromising driving performance in the hybrid architecture. This is an important aspect of the power management development.

3 Instantaneous Optimization Based Power Management

The role of power management controller in the hybrid OCPSD encompasses division of power between engine and the accumulator towards meeting a power demand at the wheels. Power demand at the wheels could be met by the engine alone, by the accumulator alone or a combination of the two. Power management at the supervisory level also dictates the operating point of the engine for a given power output in terms of its speed and torque. More specifically, the controller needs to make the following two decisions at every instant during the driving:

Distribution of power between the engine and the accumulator for a given power demand at the wheels, i.e. $P_{CE} + P_{acc} = P_{d,wh}$

Operating point of the engine, i.e. M_{CE} and ω_{CE} for a given P_{CE}

To determine the accumulator contribution P_{acc}, idea is to utilize the accumulator energy as much as possible without compromising the driving ability of the drivetrain. As pointed out earlier, pressure in the high pressure accumulator p_{HP} is an important variable that determines the driving and braking performance as well energy storage available in the accumulator. On one hand, higher accumulator pressure implies higher torque at the wheels for given unit displacements, which in turn, translates to better driving and braking ability of the drivetrain. But, higher pressure also leaves smaller room for energy storage for a given size accumulator. Moreover, constantly maintaining a high pressure in the accumulator limits its role as the auxiliary energy source on-board. Therefore, pressure in the accumulator needs to be manipulated as a function of driving conditions to fulfill the conflicting requirements of maintaining satisfactory drivability and capturing the maximum possible braking energy. The displacement of unit 2 (in the motoring mode), β_2, is set as a function of p_{HP} and expressed in the form of a look-up table. A higher p_{HP} in the accumulator above its reference level (estimated later in this section) implies larger unit 2 displacement and hence higher accumulator contribution P_{acc}. Therefore, P_{acc} can be calculated according to Eq. 5.

$$\begin{aligned} &P_{acc} = (Q_2 - Q_1)\,p_{HP} \\ \text{where, } &Q1 = \beta_i V_{1\max}\omega_i; \qquad i = 1,2 \qquad (5) \\ \text{and } &\beta_2 = f(p_{HP}) \end{aligned}$$

Braking puts up a more stringent requirement, compared to an acceleration phase, in terms of initial accumulator pressure/charge at the start of a braking sequence. In other words, manipulating the accumulator pressure by accounting for all the braking events in a drive cycle also helps the driveline provide sufficient torque at the wheels during the acceleration phases. Therefore, capturing a certain percentage of available energy at every vehicle speed has been set as the criterion for designing the accumulator pressure control. Figure 8 shows how at least 95 % of available energy in the most important speed range and 90 % elsewhere has been captured.

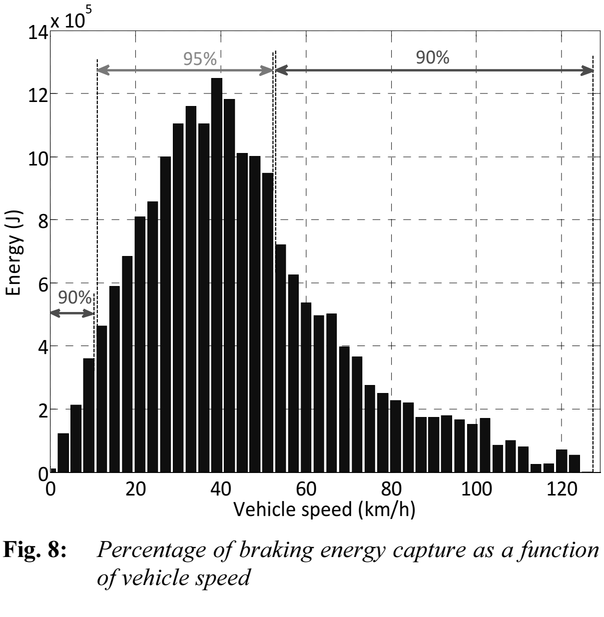

Fig. 8: *Percentage of braking energy capture as a function of vehicle speed*

To ensure that a certain percentage of available energy is captured at any vehicle speed, distribution of energy as a function of braking level or deceleration has to be considered at that speed. Figure 9, for example, shows the energy distribution at 54 km/h.

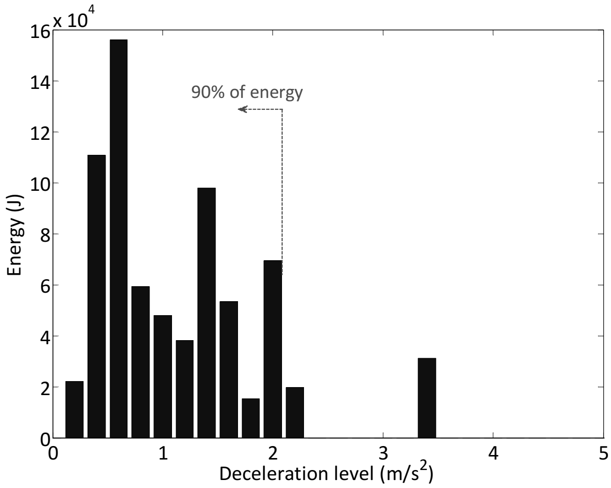

Fig. 9: *Braking energy distribution at 54 km/h vehicle speed*

As shown in Fig. 9, although there is some energy to be captured at higher deceleration levels, 90 % of it is contained within a maximum deceleration value of 2 m/s^2. Therefore, a minimum pressure level in the accumulator is selected at this speed that enables the hydraulic brakes to achieve a maximum deceleration level of 2 m/s^2 of the vehicle. To calculate the minimum required pressure, unit 2 is assumed to be at full displacement while working in the pumping mode during braking. This pressure value at 54 km/h is indicated on the plot in Fig. 10. Similar analysis is carried out at other speeds to come up with a minimum pressure profile ($p_{HP,min}$) as a function of vehicle speed, shown in Fig. 10. Since most of the braking energy is available at low and moderate vehicle speeds, a higher value of minimum accumulator pressure ensures exclusive use of hydraulic brakes. The required minimum pressure near the zero speed, really depends on the starting torque of the application. For a passenger car type of application it is moderate, but for some off-road vehicles and heavy trucks it could be significantly higher, requiring a much higher starting pressure in the accumulator.

At higher speeds, in Fig. 10, the minimum accumulator pressure drops off since there is not much energy to be captured.

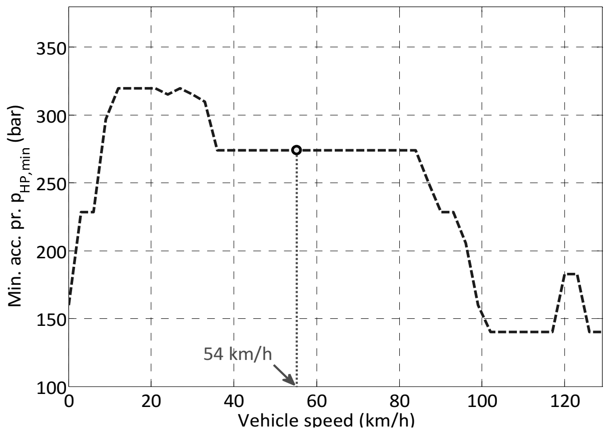

Fig. 10: *Minimum initial accumulator pressure ($p_{HP,min}$) profile*

Treating $p_{\text{HP,min}}$ as the reference pressure that must be maintained in the HP line, instantaneous optimization based power management utilizes the accumulator energy as much as possible by treating any actual pressure above its reference as available energy. Engine makes up for the difference between demanded power at the wheels and accumulator supplied power. Demanded power at the wheels is estimated from a calibration-based driver model that takes in driver's pedal and brake commands. Transmission losses involved in energy transfer from engine/accumulator to the wheels are accounted for.

The second question that needs to be addressed is that for a given power requested from the engine P_{CE}, where should the engine operate in terms of its torque and speed, M_{CE} and ω_{CE}. Here, the optimization result for the non-hybrid OCPSD has been utilized, as proposed by Kumar and Ivantysynova (2009). For a given engine power P_{CE}, the best fuel economy is obtained when the engine speed is allowed to drop along the constant power line on the engine fuel map. The minimum allowed engine speed $\omega_{\text{CE,min}}$ is limited by the condition that the transmission always operates in the power additive mode of OCPSD. Therefore, for a given wheel speed ω_{wh}, $\omega_{\text{CE,min}}$ is given by Eq. 6.

$$\omega_{\text{CE,min}} = \frac{\omega_{\text{wh}} i_{\text{axle}}}{(1 - i_0)} \tag{6}$$

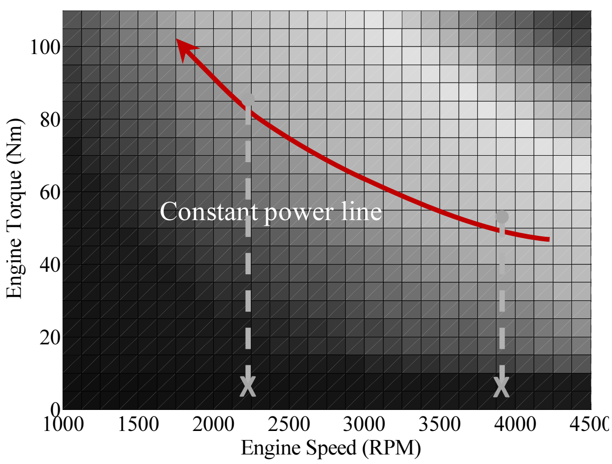

Fig. 11: *Toyota Prius engine fuel map*

It can be explained why it is most fuel efficient to operate the engine at lower speeds while fulfilling the power demanded from it. The fuel rate of Toyota Prius engine as a function of its speed and torque is shown in Fig. 11 (Rousseau et al., 2006). It can be seen from Fig. 11 that dropping to a lower speed along the constant power line also moves the engine operation to a lower specific fuel consumption region. Moving from the blue to the red region indicates less efficient engine operation.

Next, if we look at the transmission then reducing the engine speed $\omega_{\text{CE}}(\equiv \omega_{\text{B}})$ for the same wheel speed $\omega_{\text{wh}}(= \omega_{\text{A}}/i_{\text{axle}})$ has the effect of slowing down the ring gear (ω_{C}) as seen in Fig. 12.

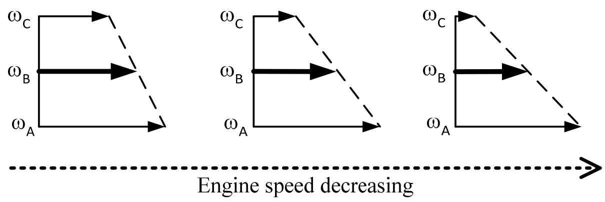

Fig. 12: *Progression to full-mechanical point*

Therefore, at the lowest allowable engine speed, transmission is close to its full-mechanical point and almost all the engine power is being transferred mechanically, making the path of power transfer very efficient (Fig. 13). Avoiding the losses involved in the hydraulic path is the key here.

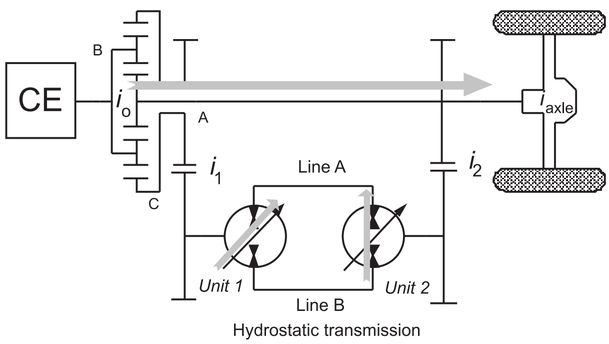

Fig. 13: *Full-mechanical point*

The net result is the engine management and efficient transmission operation taking place at the same operating condition of the powertrain, thanks to the layout of an output-coupled power-split transmission. This prompts us to utilize this result for the power management of the hybrid OCPSD. Unit 1 acts as a "loader" that loads the engine with the correct torque for the engine to output the desired torque M_{CE}. Unit 1 also maintains the pressure in HP accumulator at or above its minimum value $p_{\text{HP,min}}$ in a feedback manner. Engine throttle, which is another control input, manages the engine speed to the desired value ω_{CE} The overall schematic of the instantaneous optimization based power management controller at a supervisory

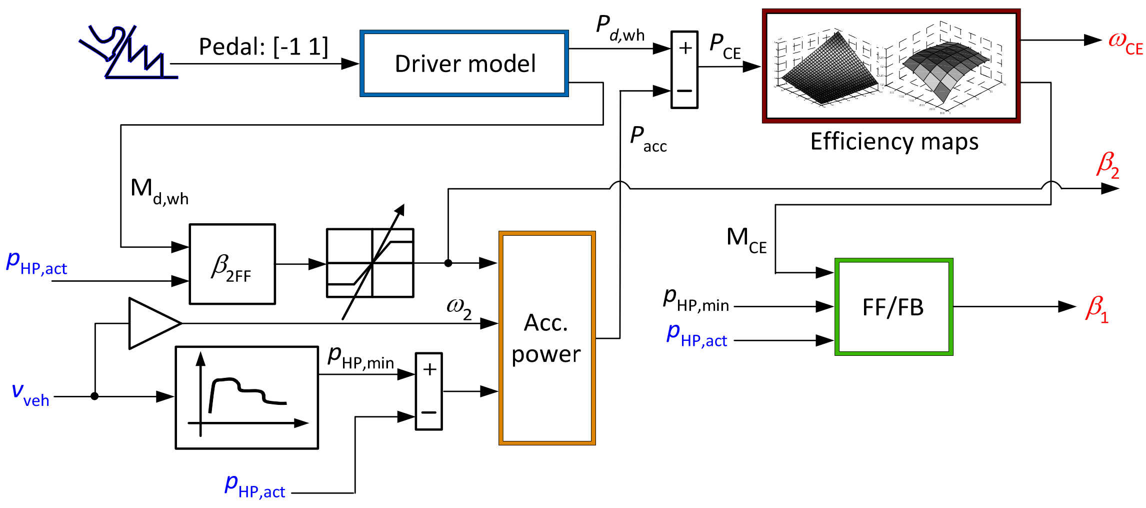

Fig. 14: *Instantaneous optimization based power management scheme*

level is shown in Fig. 14. Driver inputs in the form of accelerator and brake pedal commands are fed to the "Driver model" block that estimates the demanded power at the wheels $P_{d,wh}$. Based on the actual pressure in the HP accumulator $p_{HP,act}$ and the vehicle speed v_{veh}, unit 2 determines the power output from the accumulator P_{acc}. To decide the accumulator contribution P_{acc}, unit 2 displacement β_2 is controlled in such a way that pressure in the accumulator $p_{HP,act}$ never drops below its reference value $p_{HP,min}$ while trying to meet the demanded power at the wheels, $P_{d,wh}$. After accounting for the transmission losses, engine power output P_{CE} is estimated that together with the accumulator power P_{acc} meets the power demand at the wheels $P_{d,wh}$. Estimated engine power is sent as an input to an optimization block that contains the efficiency maps of the hydraulic units and the fuel map of the engine. Outputs of the optimization block are commanded engine speed ω_{CE} and engine torque M_{CE}. Commanded engine speed is sent to a local engine speed controller (not shown in Fig. 14) whereas the torque goes to the unit 1 displacement control block. Primary function of unit 1 is to load the engine with the correct torque as pointed out earlier. Commanded displacement values of both the hydraulic units β_1 and β_2 are sent to local displacement controllers (not shown in Fig. 14). The accumulator is assumed to be 95 % efficient.

For the purpose of direct comparison with Prius in terms of fuel economy, a Prius engine model has been used in hydraulic hybrid simulations (Rousseau et al., 2006). The 1.5L gasoline engine used in Prius is based on the Atkinson cycle with maximum power rating of 57 kW @ 5000 rpm and a peak torque rating of 115 Nm @ 4200 rpm. Simulations were run for some standard drive cycles under instantaneous optimization based control. Simulated fuel mileage in liters per 100 km (L/100 km) for a OCPSD based hydraulic hybrid passenger car, equipped with a Prius engine, is shown in Table 2.

Table 2: Fuel economy for standard drive cycles

Fuel mileage	UDDS	Highway	European
(L/100 km)	4.2	4.7	4.35

As seen from Table 2, simulated fuel economy of a OCPSD based hydraulic hybrid car is higher than the published fuel economy of Prius (Fuel Economy).

4 Experimental Validation

4.1 Experimental Set-up

In parallel to the development of theoretical aspects of the research work outlined in this paper, a 180 kW hybrid OCPSD test-rig for a class 6 application has been set-up as part of an industry sponsored project. Project scope included verifying the proposed control concepts by comparing simulation and experimental results for a class 6 vehicle type. Due to the classified nature of the project, details about the units' sizes, units' type and gear ratios cannot be revealed but architecture-wise the set-up is that of a hybrid OCPSD.

The test-rig circuit, complete with all the electrical connections needed for controls (sensors, actuators) and data acquisition, is shown in Fig. 15. Two 180 cc secondary controlled axial piston hydraulic units (Rexroth A4VSO-180) act as the engine and the load simulators. One of the many advantages of operating under secondary control is fast dynamics that enables testing of a wide range of engine characteristics and drive cycles. This test-rig can also be seen as a Hardware-in-The-Loop (HIL) set-up where engine and the load are being simulated and the transmission hardware constitutes the real part of the plant. An xPC Target platform equipped with necessary communication hardware (A/D, D/A converters) supports the real-time control implementation and fault monitoring. Instantaneous optimization based power management proposed in this work has been implemented on the test-rig and measured data are collected for a sample drive cycle.

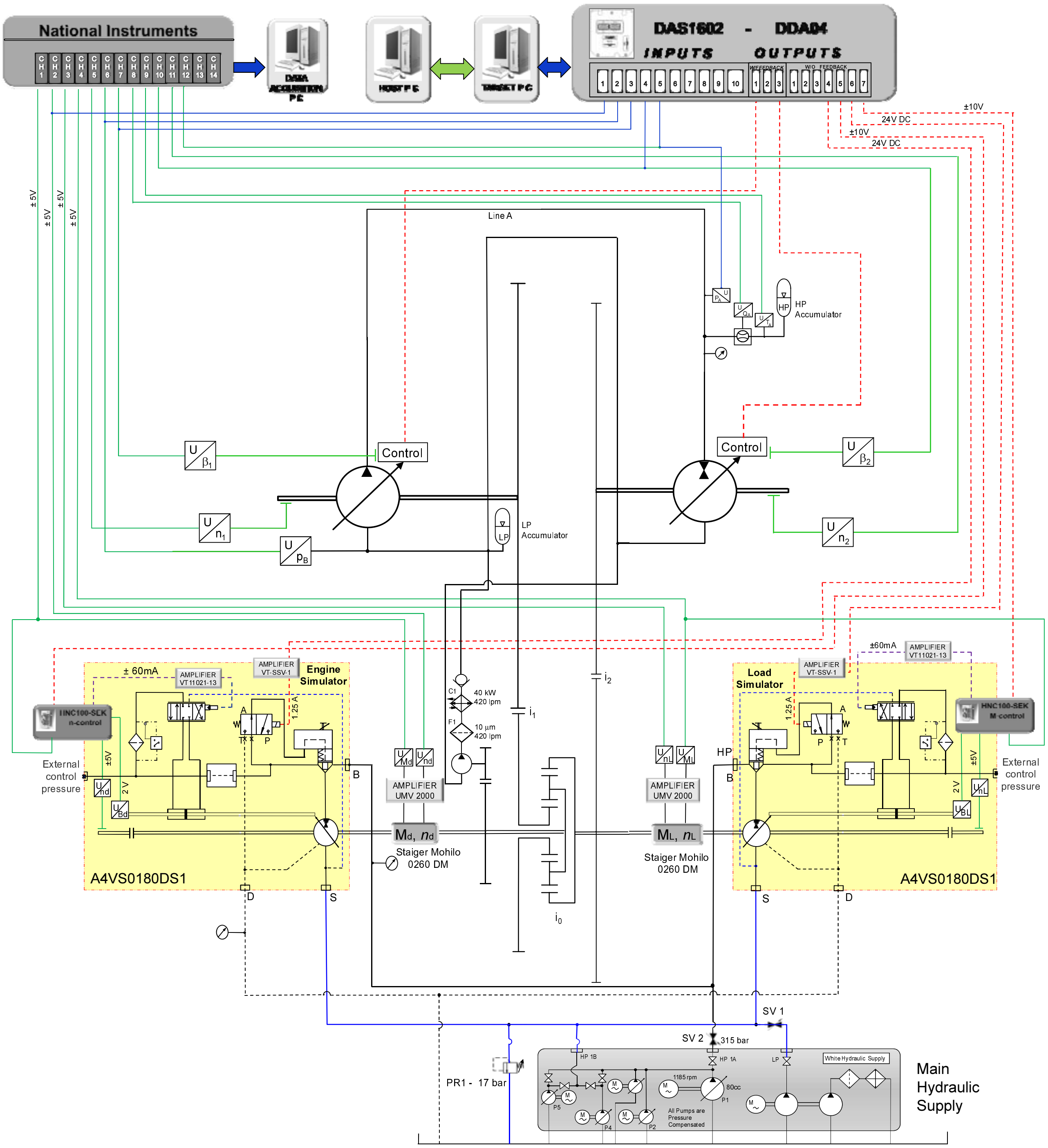

Fig. 15: *Powertrain test-rig circuit*

4.2 Comparison of Results

For the purpose of verifying the proposed power management strategy through the measurements, a sample drive cycle was chosen that consists of cruising at relatively low and high speeds as well as braking and ensuing acceleration to demonstrate the advantages associated with hydraulic hybrids. Figure 16 compares the simulation and measurement results side-by-side for all the important variables. First looking at the displacement of hydraulic units, unit 2 acts as a motor and assists the engine whenever there is sufficient charge available in the accumulator. Unit 1 loads the engine with the required torque and also maintains the pressure in the accumulator at or above its reference level. During braking, unit 2 acts as a pump by going overcenter and fills up the accumulator (170 - 180 s, 200 - 220 s). It is equivalent to hydraulic braking. Friction braking might be needed in certain scenarios when hydraulic braking alone is not sufficient. A charged accumulator meets the power demand at the load during subsequent acceleration by discharging (180 - 190 s, 225 - 250 s). The engine supplies any extra power needed during propulsion to make up for the deficit. As seen from the

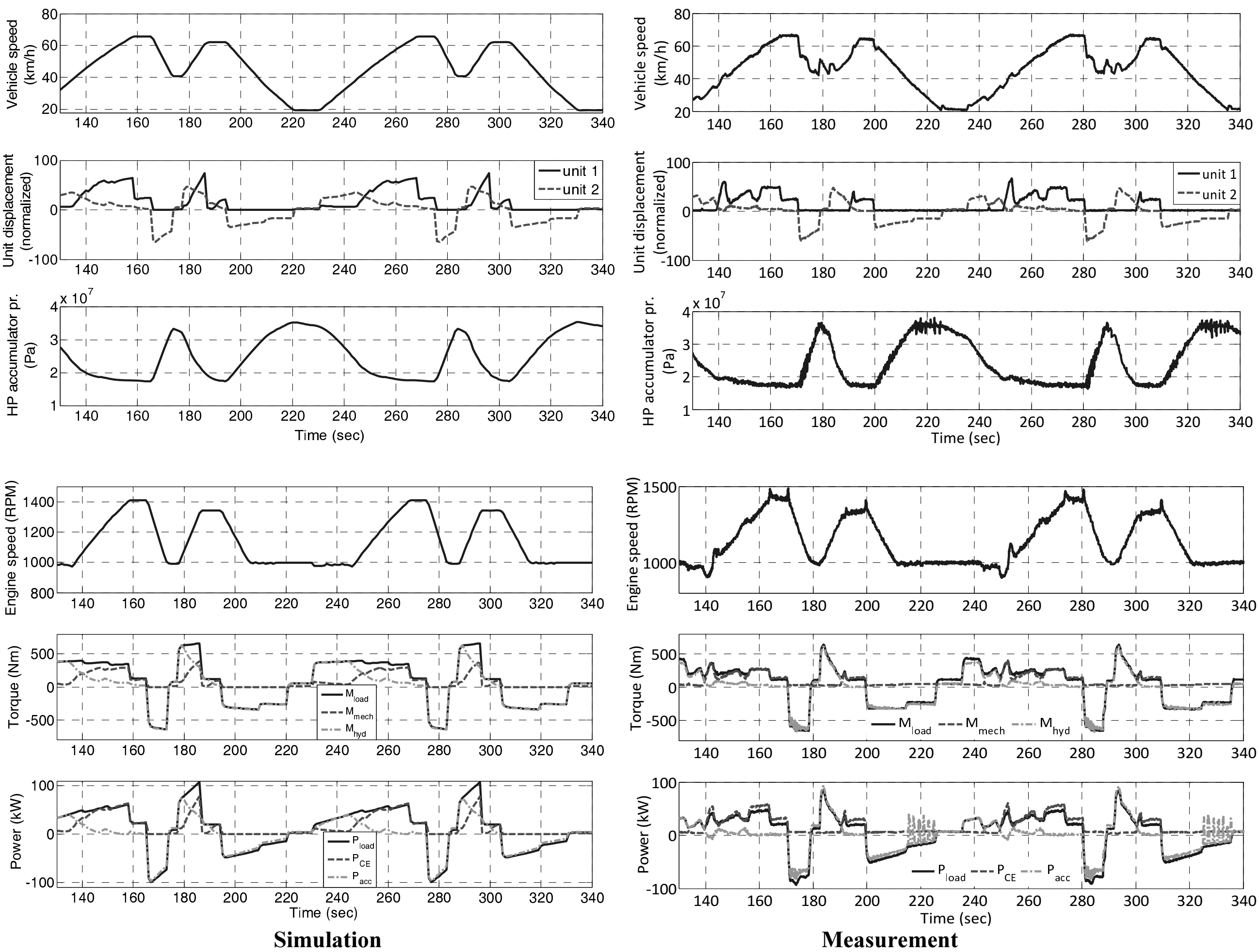

Fig. 16: *Comparison of results*

torque and power plots, accumulator is assisting the engine in meeting the demand at the load at every instant during the drive cycle. During the initial phases of acceleration following a braking event, when there is enough hydraulic power available, accumulator alone drives the load with engine just idling. It can be thought of as “hydraulic launch”. Once the HP accumulator pressure falls to its reference value, engine is the only source powering the load as seen in the last phases of acceleration and during the periods of high speed cruising (150 - 170 s, 190 - 200 s). The fluctuations seen in the pressure and accumulator power plots (215 - 225 s, 325 - 335 s) are due to the pressure relief valve opening and closing at its threshold value. The slight discrepancy seen in the load torque and power plots is due to the actual speed of the load simulator not exactly following the speed profile during hard acceleration after braking (180 - 190 s, 290 - 300 s). This drop in actual acceleration creates a lower torque and power demand at the load. Therefore, unit 1 displacement stays at a lower value to enable the engine unit to meet a lower than expected torque demand at the load. This drive cycle was created to test the engine and load simulators close to their acceleration and torque limits. For a drive cycle with moderate demands from these two units, match between simulation and measurements is expected to be closer.

5 Conclusions

The main aim of this paper is to propose a power management strategy to minimize fuel consumption in hydraulic hybrids. Sizing the hydraulic accumulator for a specific application has implications beyond compactness and weight of the powertrain. A bigger accumulator, for example, allows maintaining a higher minimum pressure for the given amount of energy storage, which in turn, has an influence on the driving performance of the powertrain. A smaller accumulator, on the other hand, needs more careful manipulation of the pressure to achieve the dual objective of maximizing the energy capture and meeting the driving performance. A procedure for sizing the accumulator has been illustrated for OCPSD based hybrid but it is quite general in nature and is applicable for any other configuration, such as series or parallel, based hybrid.

To realize the goal of minimizing the fuel consumption without compromising the performance, system pressure is identified as the most important variable. Instantaneous optimization based power management, at every instant, seeks to manipulate the pressure in such a way that ensures maximum utilization of accumulator energy without any drop in driving ability of the powertrain. In addition, it also achieves engine management for a given engine power output by operating the transmission in a purely mechanical mode and thus making the path of energy transfer very efficient. High efficiency of transmission concurrent with optimal operation of the engine is a feature afforded by the layout of OCPSD.

Hybrid OCPSD was simulated for some standard drive cycles with the instantaneous optimization based control and the result indicated fuel economy numbers much higher than ones reported for conventional powertrains in all driving scinarios.

Experimental validation of the proposed power management comes from the data collection on a powertrain test-rig built on the HIL principle. Simulation and measurement data for a drive cycle match closely for many system variables. Ease of implementation and the practicality of the approach have been proved by real-time control and data collection.

Nomenclature

A	Sun gear	-
B	Carrier gear	-
C	Ring gear	-
E_{acc}	accumulator energy	[J]
E_b	braking energy	[J]
E_{cap}	recoverable braking energy	[J]
F	force	[N]
$M_{br,wh}$	braking torque at the wheels	[Nm]
M_{CE}	engine torque	[Nm]
$M_{d,wh}$	demanded torque at the wheels	[Nm]
P_{acc}	accumulator power	[W]
P_{CE}	engine power	[W]
$P_{d,wh}$	demanded power at the wheels	[W]
Q_1	flow rate of unit 1	[m^3/s]
Q_2	flow rate of unit 2	[m^3/s]
i_{axle}	differential gear ratio	-
i_0	standing gear ratio	-
i_1	gear ratio between ring and unit 1	-
i_2	gear ratio between sun and unit 2	-
n	polytropic index	-
p	pressure	[Pa]
p_{HP}	pressure in HP accumulator	[Pa]
r	pressure ratio	-
r_{tire}	tire radius	[m]
V	gas volume	[m^3]
$V_{1,max}$	max. displacement volume of unit 1	[m^3/rad]
$V_{2,max}$	max. displacement volume of unit 2	[m^3/rad]
v_{veh}	vehicle velocity	[m/s]
β_1	unit 1 displacement (normalized)	-
β_2	unit 2 displacement (normalized)	-
$\beta_{2,FF}$	feedforward unit 2 displacement	-
ω_1	unit 1 shaft speed	[rad/s]
ω_2	unit 2 shaft speed	[rad/s]
ω_A	sun speed	[rad/s]
ω_B	carrier speed	[rad/s]
ω_C	ring speed	[rad/s]
ω_{CE}	engine shaft speed	[rad/s]
ω_{wh}	wheel rotational speed	[rad/s]

	Subscripts
FF/FB	feedforward/feedback
act	actual
br	braking
fric	friction
min	minimum
wh	wheel

References

ARTEMIS. 2006. http://www.artemisip.com/Heddat2.htm

Bowns, D. E., **Vaughan, N. D.** and **Dorey, R. E.** 1981. Design Study of a Regenerative Hydrostatic Split Power Transmission for a City Bus. *IMechE Hydrostatic Transmissions for Vehicle Application*, pp. 29 - 38, Coventry, England.

Davies, A. S. 1989. *The Reduction of City Bus Exhaust Emissions by Means of a Regenerative Powertrain*. SAE paper 890267.

Dorey, R. E. and **Vaughan, N. D.** 1984. Computer Aided Design of Split Power Hydrostatic Transmission Systems. *IMechE, Vol. 198B, No. 2*, pp. 61 - 69.

EPA. 2006. http://www.epa.gov/oms/technology/420f06054.pdf

Fuel Economy. http://www.fueleconomy.gov/feg/noframes/19813.shtml

Hugosson, C. 1993. Cumulo Hydrostatic Drive – A Vehicle Drive with Secondary Control. *Third Scandinavian International Conference on Fluid Power*, Linkoping, Sweden.

Kumar, R. and **Ivantysynova, M.** 2009. An Optimal Power Management Strategy for Hydraulic Hybrid Output Coupled Power-Split Transmission. *Bath ASME Symposium on Fluid Power and Motion Control*. [DSCC2009-2780]. Hollywood, USA.

Martini, S. 1984. *The M.A.N. Hydrobus:* A Drive Concept with Hydrostatic Brake Energy Recovery. *International Symposium on Advanced and Hybrid Vehicles*.

Nakazawa, N., **Kono, Y.**, **Takao, E.** and **Takeda, N.** 1987. Development of a Braking Energy Regeneration System for City Buses. *SAE paper 872265*.

Renius, K. T. and **Resch, R.** 2005. Continuously Variable Tractor Transmissions. ASAE Distinguished Lecture Series No. 29. pp. 1 - 37. *Agricultural Equipment Technology Conference*, Louisville, KY, USA.

Rousseau, A., **Kwon, J.**, **Sharer, P.**, **Pagerit, S.** and **Duoba, M.** 2006. Integrating Data, Performing Quality Assurance, and Validating the Vehicle Model for the 2004 Prius Using PSAT. *SAE paper 2006-01-0667*, SAE World Congress, Detroit.

Rajneesh Kumar
Born on July 2nd 1980 in Dehri-on-Sone, Bihar (India). He received his B.Tech. Degree from Indian Institute of Technology Madras (IITM), India, in Mechanical Engineering in 2002. He worked as a Systems Engineer for two years before coming to Purdue University in 2004. He received his MS and PhD Degrees at Purdue University, USA, in Mechanical Engineering in 2006 and 2010 respectively. He is currently a Systems Control Engineer at Parker Hannifin Corp. His main areas of interest are power management of hydraulic hybrid powertrains, efficient hydraulic systems and control of fluid power systems.

Monika Ivantysynova
Born on December 11th 1955 in Polenz (Germany). She received her MSc. Degree in Mechanical Engineering and her PhD. Degree in Fluid Power from the Slovak Technical University of Bratislava, Czechoslovakia. After 7 years in fluid power industry, she returned to university. In April 1996 she received a Professorship in fluid power & control at the University of Duisburg (Germany). From 1999 until August 2004 she was Professor of Mechatronic Systems at the Technical University of Hamburg-Harburg. Since August 2004 she is Professor in Mechanical Engineering and Agricultural and Biological Engineering at Purdue University, USA. She was approved as Maha named Professor in Fluid Power Systems and director of the Maha Fluid Power Research Center at Purdue University in November 2004. Her main research areas are energy saving actuator technology and model based optimization of displacement machines as well as modeling, simulation and testing of fluid power systems. Besides the book “Hydrostatic Pumps and Motors” published in German and English, she has published more than 90 papers in technical journals and at international conferences.